



# An ANN-adaptive dynamical harmony search algorithm to approximate the flyrock resulting from blasting

Mahdi Hasanipanah<sup>1</sup> · Behrooz Keshtegar<sup>2,3</sup> · Duc-Kien Thai<sup>4</sup> · Nguyen-Thoi Truong<sup>2,3</sup>

Received: 4 June 2020 / Accepted: 3 July 2020 / Published online: 13 July 2020  
© Springer-Verlag London Ltd., part of Springer Nature 2020

## Abstract

Blasting is the cheapest and most common method of rock excavation. The basic purpose of blasting is to breakage and displacement of rock mass and, on the other hand, it has some undesirable and inevitable effects such as flyrock. In this study, a novel hybrid artificial neural network (ANN) based on the adaptive musical inspired optimization method is proposed for accurate prediction of blast-induced flyrock. The dynamical adjusting process was adaptively introduced to enhance the ability of harmony search algorithm to obtain the optimum relationship between input variables, i.e., spacing, burden, stemming, powder factor and density of rock and output variable, i.e., flyrock. Two adjusting processes were used to update the new position of particles. The statistical information of the harmony memory was implemented in the proposed hybrid ANN coupled with adaptive dynamical harmony search (ANN-ADHS). The capacity for agreement, tendency, and accuracy of the proposed ANN-ADHS was compared with that of the ANN and two hybrid ANN models coupled by harmony search (ANN-HS) and particle swarm optimization (ANN-PSO) models using comparative statistics such as root mean square error (RMSE). The results confirmed viability and effectiveness of the ANN-ADHS model (with RMSE = 17.871 m and correlation coefficient ( $R^2$ ) = 0.929) and showed its capacity for better predictive performance compared to ANN-HS (with RMSE = 22.362 m and  $R^2$  = 0.871), ANN-PSO (with RMSE = 24.286 m and  $R^2$  = 0.832), and ANN (with RMSE = 24.319 m and  $R^2$  = 0.831).

**Keywords** Blasting · Flyrock · ANN · Adaptive dynamic harmony search · Optimization algorithms

## 1 Introduction

In general, blasting operations conducted during surface mining projects may lead to the fragmentation of overburden and exposure of ore benches [1]. During blasting operations, with every explosion, a huge quantity of energy is released in the form of heat, gas, pressure, and stress waves. Such massive energy is not completely converted into mechanical

energy for breaking the rock mass. Only 20–30% of this energy is applied to rock fragmentation and the remaining part merely goes for generating negative effects such as flyrock, ground vibration, air blast, noise, etc. (Figure 1) [2–11]. According to Trivedi et al. [3] and Little and Blair [12], flyrock is produced when the energy released by the explosion takes the least resistance path to travel. This incident can bring about serious threat to the safety of people living nearby and buildings located in the vicinity of the site [3, 13].

The most important factors that lead to flyrock event include over-charging of the blast holes, inadequate burden, insufficient stemming, imprecision in design of blast-hole patterns, anomaly in the rock structure geology, back-break, improper drilling, and carelessness [3, 14, 15]. Based on findings of Bajpayee et al. [16, 17], if the geo-mechanical strength of the adjacent rock mass is imbalanced, it results in the movement of explosive energy towards the paths, where it faces the least resistance. This condition causes flyrock to be propelled beyond the estimated blast area. According to Richards and Moore [18], basic mechanisms of flyrock

✉ Behrooz Keshtegar  
beh.keshtegar@tdtu.edu.vn

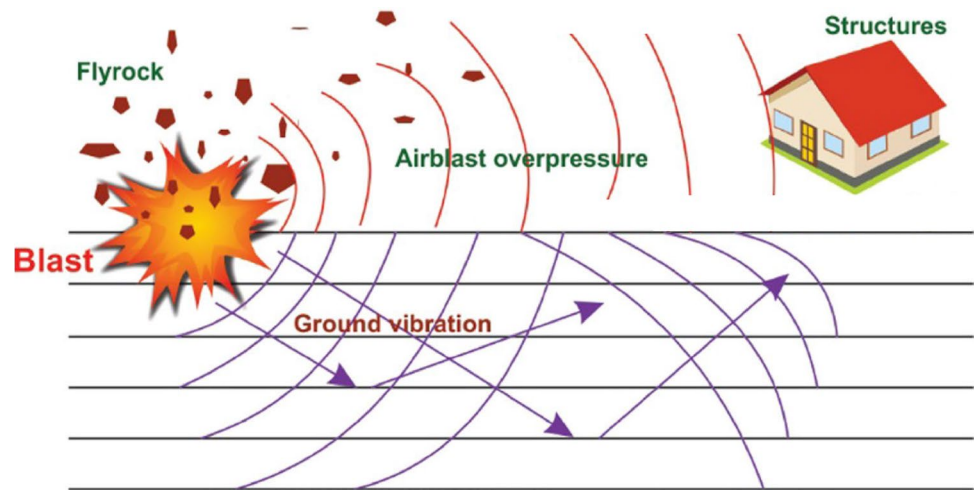
<sup>1</sup> Institute of Research and Development, Duy Tan University, Da Nang 550000, Vietnam

<sup>2</sup> Division of Computational Mathematics and Engineering, Institute for Computational Science, Ton Duc Thang University, Ho Chi Minh City, Vietnam

<sup>3</sup> Faculty of Civil Engineering, Ton Duc Thang University, Ho Chi Minh City, Vietnam

<sup>4</sup> Department of Civil and Environmental Engineering, Sejong University, 98 Gunja-dong, Gwangjin-gu, Seoul 143-747, South Korea

Fig. 1 Blasting phenomena [11]



incidence in bench blasting are cratering, rifling, and face burst. As maintained by Rehak et al. [15] and Bajpayee et al. [17], flyrock is one of the most frequent incidences causing fatal accidents in open cast mines in India. Verakis and Lobb [19] stated that flyrock and lack of security in blast region are responsible for roughly 68% of the injuries that occur in the opencast mines. On the other hand, according to Kecojevic and Radomsky [20], during the past three decades, improper blasting shelter, not evacuating the blast region from people, and insufficient guarding of the access roads have accounted for 45.64% of the fatal and non-fatal events in surface coal mining. Literature contains a number of empirical models proposed by different researchers [21, 22] for the aim of solving the intimidating problem of flyrock. The most significant drawback of these models is that they have failed to involve all factors that can have impact on the flyrock launch velocity or throw. This weakness has made them incapable of entirely solving the flyrock problem.

Today, advanced artificial intelligence (AI)-based tools are extensively applied to many situations, including the problem of decision making under uncertain conditions and with uncertain information [23–39]. AI has a stochastic characteristic that makes it effectively applicable to numerous fields of study, e.g., Information Technology, data analysis, decision making, and predictive models [40].

It is highly complex to predict flyrock, since it requires to inspect numerous variables. Consequently, literature lacks a single method that can be comprehensive enough to perform such complicated task. Every model proposed in this regard involves some variables and overlooks some others [41]. Thus, for an effective and accurate prediction of flyrock, innovative methods on the basis of AI are required. Rezaei et al. [41] introduced a fuzzy interface system (FIS) to estimate the flyrock. In another study, artificial neural network (ANN) and FIS were developed by Ghasemi et al. [42] to predict flyrock. Their findings confirmed the effectiveness of

both techniques in the flyrock estimation. To the same end, Monjezi et al. [43] integrated ANN and genetic algorithm (GA). In another project, support vector machine (SVM) and statistical models were developed by Khandelwal and Monjezi [44] for the purpose of introducing a novel model applicable to flyrock estimation. According to their results, SVM outperformed the statistical models in regard to predicting flyrock. Marto et al. [45] combined the advantages of both ANN and imperialist competitive algorithm (ICA) to have an accurate prediction of flyrock. They made use of ICA to optimize ANN. In their experiments, the hybrid ICA-ANN model worked better than ANN regarding the flyrock estimation. In another research in this field, Jahed Armaghani et al. [46] utilized the adaptive neuro-fuzzy inference system (ANFIS) to estimate flyrock, and their findings confirmed the effectiveness of ANFIS in terms of predicting flyrock. Nikafshan Rad et al. [47] integrated the recurrent fuzzy neural network (RFNN) with GA for the purpose of estimating flyrock. They also made use of ANN and a hybridized model of ANN and GA. Their findings showed that RFNN-GA could outperform ANN and ANN-GA regarding the precision level.

Lu et al. [48] presented an outlier robust extreme learning machine (ORELM) to predict flyrock, and compared its results with ANN and regression models. Their results confirmed the acceptability of the proposed ORELM model in this field. A biogeography-based optimization (BBO) algorithm was combined with ELM to predict flyrock in the study conducted by Murlidhar et al. [49]. In their study, the particle swarm optimization (PSO) algorithm was also used to train ELM. They concluded that the accuracy of the BBO-ELM model was better than PSO-ELM and ELM models. Han et al. [50] offered the random forest (RF) model to select the most effective parameters on the flyrock. Then, they used a Bayesian network (BN) to develop a probabilistic predictive model to predict flyrock. Their results showed

the effectiveness of RF and BN models in the flyrock prediction field. In another study conducted by Zhou et al. [51], the Monte Carlo (MC) simulation and nonlinear models were implemented to estimate the flyrock distance. Their analyses indicated the superiority of the proposed models in predicting the flyrock. The multiple discriminant analysis (MDA) model was developed by Hudaverdi and Akyidiz [52] to predict flyrock. According to their results, the MDA model can be introduced as a new and reliable model to predict blast-induced flyrock. Recently, Jahed Armaghani et al. [53] predicted the flyrock using a combination of gray wolf optimization (GWO) and support vector regression (SVR). In addition, two models, including multivariate adaptive regression splines (MARS) and principle component regression (PCR), were used for comparison aims. They showed that GWO was an excellent algorithm to improve the SVR performance, and its accuracy was found better than the MARS and PCR models.

In the present paper, a novel ANN coupled with adaptive dynamical harmony search (ANN-ADHS) is proposed to predict flyrock. The capability of ANN-ADHS is compared with the ANN and two hybrid ANN models coupled by the harmony search (ANN-HS) and PSO (ANN-PSO) models. To the best of our knowledge, any research has not as yet tested the efficiency of ANN-ADHS model in predicting the flyrock in different time scales.

## 2 Data for modeling process

To achieve the objectives defined for this study, a field study was conducted at three quarry sites of granite rock located near the city of Johor, Malaysia, including the Ulu Tiram, Pengerang, and Masai quarry sites (see Fig. 2). In all of the above-mentioned sites, rock strength ranges between 30 and 110 MPa. The aggregate applied to construction purposes is produced in these sites using the drilling and blasting methods. The blast holes used are of the size of 75, 115, and 150 mm in diameter.

The explosive material mainly applied to blasting operations is ammonium nitrate/fuel oil (ANFO) as well as dynamite that is generally utilized for blast initiation. To stem the blast holes, fine gravels are used in these sites. In all the sites, flyrock inevitably takes place; thus, an accurate estimation of flyrock for controlling the negative environmental impacts is of high importance. To this end, 82 blasting operations were inspected for the aim of measuring the five most effective variables on flyrock, i.e., spacing, burden, stemming, powder factor, and density. For each blast, the bench surface was colored, and to check the projection of flyrock, three video cameras were installed. Next, the videos were checked to determine the locations of the maximum rock projections; the flyrock distances were then measured using a measuring tape. In the modeling processes of the proposed models, the gathered datasets were divided into training (80% of the whole datasets) and testing (20% of



Fig. 2 View of the fields investigated in this research

the whole datasets) datasets. The statistical properties of the data for modeling process is listed in Table 1. Furthermore, Fig. 3 shows the sensitivity degree of input parameters on the output (flyrock). This figure shows that the spacing (with 36%) and powder factor (with 27%) are the most sensitivity parameters on the flyrock in the studied cases.

### 3 Hybrid ANN model crumpled by ADHS

The input variables presented in Table 1 are utilized to provide a nonlinear relation for flyrock distance. The ANN model is used to connect input variables into flyrock distance as output variable with a nonlinear mathematical form. ANN can provide a nonlinear relation using three layers, i.e., input, hidden, and output layers, which are plotted in Fig. 4. In ANN, the nonlinear function is defined based on the following relations [54]:

$$Y = b + \sum_{j=1}^M w_j \phi_j$$

$$\phi_j = \frac{1}{1 + \exp[-(b_j + \sum_{i=1}^n w_{ji} x_i)]}$$
(1)

where  $b$  and  $b_j$  represent bias for output and the  $j$ -th hidden node, respectively,  $w_j$  and  $w_{ji}$ , respectively, denote weights for output and hidden nodes which are used to connect the  $j$ -th hidden node to output node and to connect the  $i$ -th input node to the  $j$ -th hidden node, respectively, and  $\phi_j$  represents nonlinear map as sigmoid function that is utilized for transferring the  $j$ -th hidden node. As can be seen in Fig. 2, the  $M$ -neuron in hidden layer can provide a nonlinear relation using the sigmoid function in this study.

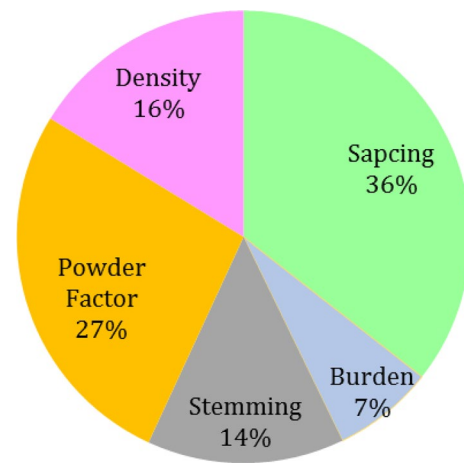


Fig. 3 Sensitivity degree of input variables on the output (flyrock)

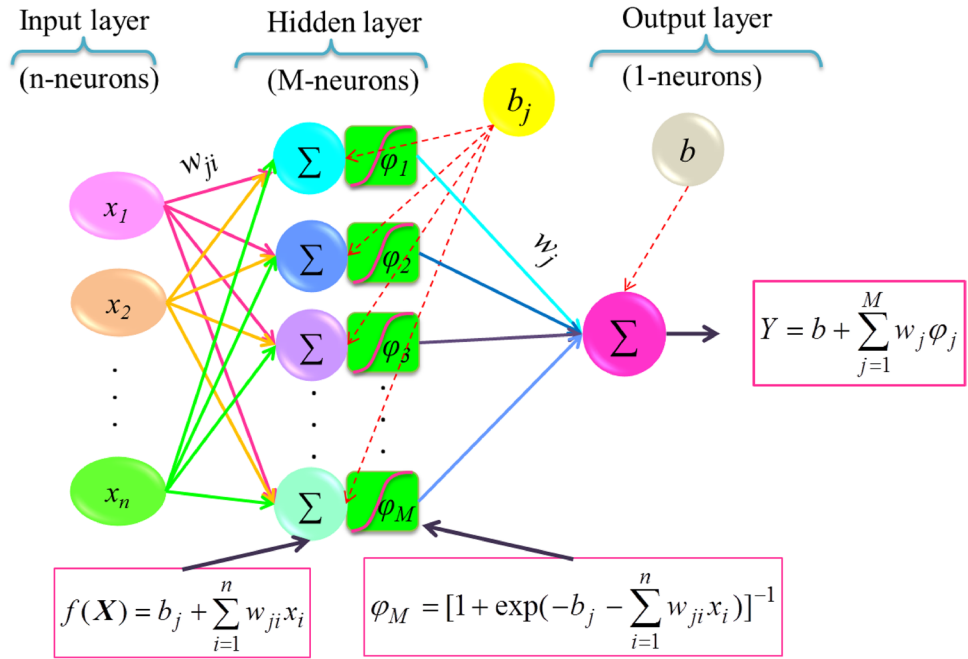
The capability of the ANN model strongly depends on the weights ( $w_j$  and  $w_{ji}$ ) and biases ( $b$  and  $b_j$ ). Consequently, providing the best connection between input and output layers causes the highest capacity for an accurate and robust prediction, which is obtained by optimum conditions of weights and biases. Therefore, the learning approach plays a vital role in establishing a robust and accurate model. The back-propagation (BP) approach of MLNN is a popular training method applicable to determining the weights and biases. The metaheuristic optimization methods can be used to train ANN [55–59] for searching optimum coefficient vector of weights and biases  $\theta = [b, w]$ . The ANN can be trained using optimization algorithms by minimizing the error between the observed and predicted data as below [55]:

**Table 1** Statistical properties of the data for modeling process in the testing and training phases

Variables	Train (56 data)							
	Xmin	Xmax	Mean	STD	COV	Skewness	R	
Spacing (m)	2.65	3.9	3.368	0.422	0.125	-0.417	-0.716	
Burden (m)	1.5	3.15	2.371	0.495	0.209	0.314	0.097	
Stemming (m)	1.7	3.6	2.160	0.406	0.188	1.708	0.018	
Powder Factor (kg/m <sup>3</sup> )	0.67	1.05	0.877	0.115	0.132	0.010	-0.206	
density (g/cm <sup>3</sup> )	2.3	2.8	2.576	0.166	0.065	-0.254	0.143	
Flyrock Distance (m)	61	324	213.684	67.780	0.317	-0.534	1	
	Test (26 data)							
Spacing (m)	2.65	4.000	3.23	0.401	0.124	0.233	-0.395	
Burden(m)	1.95	3.2	2.522	0.420	0.167	0.050	-0.129	
Stemming(m)	1.7	3.3	2.198	0.392	0.178	1.207	-0.421	
Powder Factor(kg/m <sup>3</sup> )	0.67	1.05	0.9216	0.106	0.115	-0.723	-0.634	
density (g/cm <sup>3</sup> )	2.3	2.8	2.582	0.174	0.067	-0.345	0.364	
Flyrock Distance (m)	173	334	246.84	47.745	0.193	0.225	1	



**Fig. 4** Structure of the ANN model for flyrock prediction



$$\min MSE = \frac{1}{N} \sum_{i=1}^M [O_i - Y_i]^2, \tag{2}$$

where  $N$  and  $O$  are the number of training data and observed flyrock, respectively. In this work, a novel hybrid AI-based ANN coupled with an optimization algorithm using adaptive music-inspired approach is proposed for approximating the flyrock.

In ADHS, a modified adjusting approach is presented based on the information of harmony memory at every iteration. The new position of harmony elements is dynamically updated using two random adjusting procedures. Through the first procedure, the harmony elements are adjusted using the maximum and minimum values for each random variable in harmony memory by a dynamic harmony memory considering rate (HMCR), which is computed as follows:

$$HMCR(k) = 0.95 + 0.1 \times \sqrt{\frac{k}{NI} - (\frac{k}{NI})^2}, \tag{3}$$

where  $k$  is the current iteration and  $NI$  is the total number of iterations. Whereas, the best memory of the variable is tuned using an adjusting step size, which is computed based on the information of harmony elements through the second random procedure. Through the second adjusting procedure, the dynamical pitch adjusting rate (PAR) is used to adopt the best harmony memory as follows:

$$PAR(k) = 0.3 + 0.6 \times [1 - \sqrt{1 - k/NI}]. \tag{4}$$

Using two dynamical relations presented in Eqs. (3) and (4), the new updating position for unknown coefficient vector is randomly given by the following schemes:

$$\theta_{new} = \begin{cases} \theta_{old} \pm \gamma(k) \times bw_i(k) & r_1 \leq HMCR(k) \\ \theta_L + r_3 \times (\theta_U - \theta_L) & r_1 > 1 - HMCR(k) \end{cases} \tag{5}$$

$$\theta_{new} = \begin{cases} \theta_{old} \pm \gamma(k) \times [\theta_i^{max} - \theta_i^{min}] & r_2 \leq PAR(k) \\ \theta_L + r_3 \times (\theta_U - \theta_L) & r_2 > 1 - PAR(k) \end{cases}, \tag{6}$$

where  $\theta_{old}$  and  $\theta_{new}$  denote the old and new elements of harmony memory, respectively.  $r_1, r_2, r_3 \in [0, 1]$  are random numbers between 0 and 1.  $\theta_i^{max}$  and  $\theta_i^{min}$  are maximum and minimum coefficients, respectively, for the  $i$ -th input variable in the harmony elements.  $\theta_U$  and  $\theta_L$ , respectively, denote upper and lower bounds of unknown coefficients, where  $\theta_U = 1$  and  $\theta_L = -1$ . In Eq. (5),  $bw(k)$  and  $\gamma(k)$  are the dynamical bandwidth and controlling factor, respectively, proposed by the following relations:

$$bw_i(k) = \frac{\theta_i^{max} - \theta_i^{min} + 0.0001}{10} \exp\left[-\frac{10k}{NI}\right] \tag{7}$$

$$\gamma(k) = \sqrt{1 - \frac{k}{NI}}, \tag{8}$$

where  $\exp$  represents the exponential operator. In Eq. (7),  $bw_i(k)$  is computed based on information of the harmony memory such as maximum and minimum harmony elements. The dynamical bandwidth is decreased based on the

increment of iterations, while it is controlled by the factor  $\gamma(k)$  at the final iteration. During the second adjusting process using Eq. (6), the movement of each harmony from the previous position is controlled by the coefficient  $\sqrt{1 - k/NI}$ . Therefore, a smaller value is given for  $\gamma(k) \times [\theta_i^{\max} - \theta_i^{\min}]$  at the final iteration; thus, a fixed position is obtained using this adjusting process. Unlike HS, the new position for harmony elements of the unknown coefficients is adjusted using two random steps with dynamical parameters. The algorithm of HS formulated by adjusting processes using Eqs. (5) and (6) is presented as follows:

are compared with those of the traditional ANN model with  $M=7$ , ANN coupled with harmony search (HS) optimization (ANN-HS) with parameters of  $HMS=10$ ,  $M=7$ ,  $NI=2000$ ,  $HMCR=0.95$ ,  $PAR=0.35$ , and  $bw=0.005$ , and particle swarm optimization (PSO) with particle size of 10,  $M=7$ ,  $NI=2000$ ,  $c_1=c_2=2$ ,  $\eta_{\max}=0.9$ ,  $\eta_{\min}=0.3$ ,  $V_0=0.3r$  and  $\theta_0=1-2r$  [59].

---

### Algorithm ADHS for adjusting the new elements of harmony memory

---

**Find maximum ( $\theta_i^{\max}$ ) and minimum ( $\theta_i^{\min}$ ) elements**

**Determine the dynamical PAR and HMCR**

**Compute the dynamical bandwidth and  $\gamma$**

**IF**  $r_1 \leq HMCR(k)$  **THEN**

$$\theta_{new} = \theta_{old} \pm \gamma \times bw_i(k) ;$$

**IF**  $r_2 \leq PAR(k)$  **THEN**

$$\theta_{new} = \theta_{old} + \gamma \times [\theta^{\max} - \theta^{\min}] ;$$

**ENDIF ELSE**

$$\theta_{new} = \theta_L + r_3 \times (\theta_U - \theta_L) ;$$

**ENDIF**

---

The framework for training the ANN models using the ADHS optimization process is presented in Fig. 5. As can be seen in this figure, this method can be applied simply with three random strategies to update the new harmony elements: selection from the design domain, adjustment using HMCR, and adjustment using PAR factors. In the current study, this framework is used in a MATLAB code with number of harmony memory size (HMS) of 10, hidden nodes of  $M=7$ ,  $NI=2000$ , and  $\theta_0=1-2r$ , i.e.,  $r \in [0, 1]$ . The predicted results obtained by the proposed ANN-ADHS

## 4 Results and discussion

The accuracy and agreements of the proposed hybrid AI-based adaptive music-inspired intelligent models are compared with those of ANN, ANN-HS, and ANN-PSO using five comparative statistics, i.e., the mean absolute error (MAE), root mean square error (RMSE), modified agreement index ( $d$ ), and modified Nash and Sutcliffe efficiency (NSE) and maximum relative errors (ax (RE)). This error matrix is

**Fig. 5** Framework of ANN-ADHS for training the AI-based data driven model

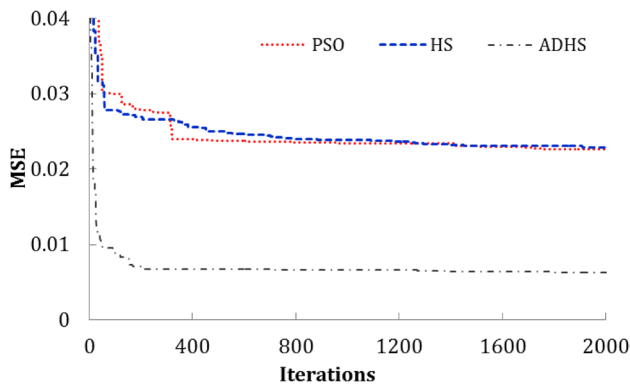
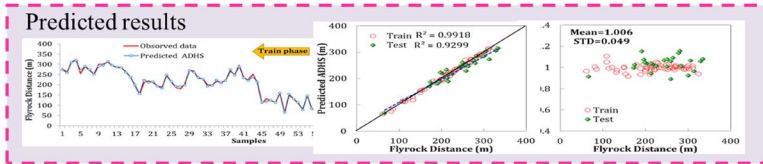
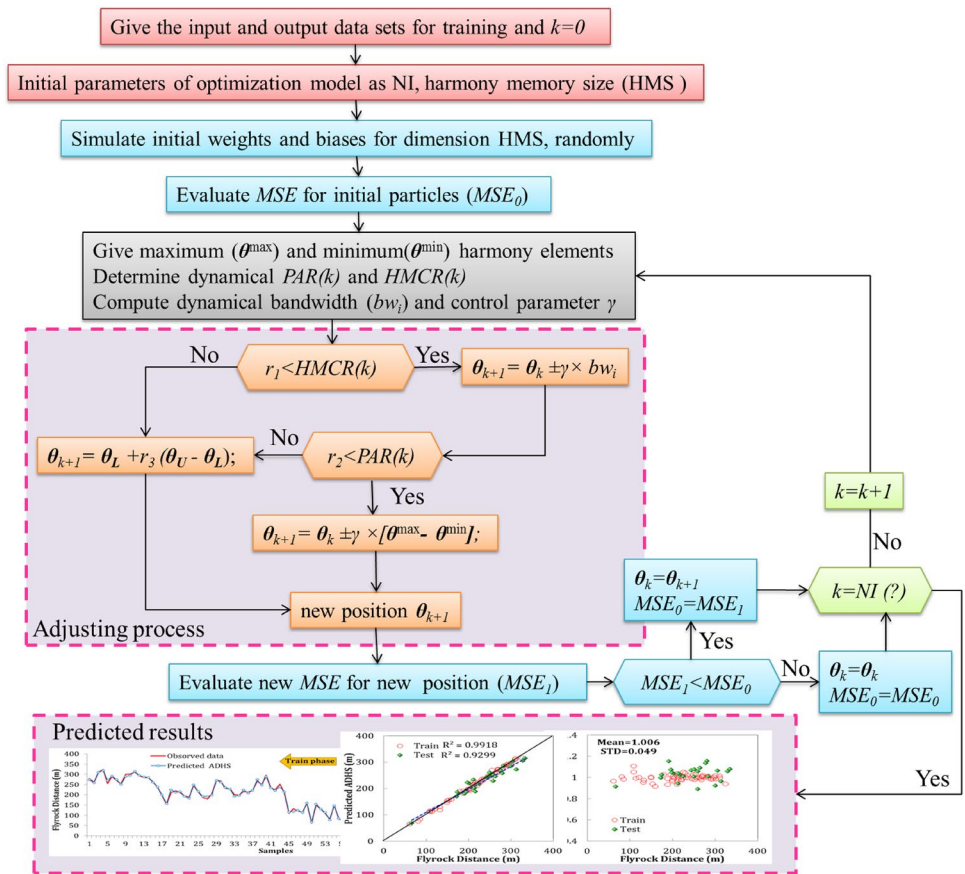


**Fig. 6** MSE of different optimization methods for training the ANN models

implemented to illustrate the agreement and accuracy level of the proposed models. The comparative statistics were evaluated using the following relations [60–72]:

$$RMSE = \sqrt{\frac{1}{N} \sum_{i=1}^N [S_i - Y_i]^2} \tag{9}$$

$$MAE = \frac{1}{N} \sum_{i=1}^N |S_i - Y_i| \tag{10}$$

$$d = 1 - \frac{\sum_{i=1}^N |S_i - Y_i|}{\sum_{i=1}^N |S_i - \bar{S}| + |Y_i - \bar{S}|}, \quad 0 < d \leq 1 \tag{11}$$

$$NSE = 1 - \frac{\sum_{i=1}^N |S_i - Y_i|}{\sum_{i=1}^N |S_i - \bar{S}|}, \quad -\infty < NSE \leq 1 \tag{12}$$

$$Max(RE) = \max \left\{ \frac{|S_i - Y_i|}{S_i} \times 100, i = 1, 2, \dots, N \right\} \tag{13}$$

where  $N$  denotes the number of data,  $S_i$  and  $Y_i$  are the  $i$ -th data points for the observed and predicted sets, respectively, and  $\bar{S}$  stands for the average of observed data points. The  $RMSE$  and  $MAE$  values for each model are tended to zero; thus, it can be said that the predicted model provides accurate predictions with minimum errors. In Eq. (11),  $d$

**Table 2** Comparative statistics for different ANN models in the training and testing phases

Methods	Train					Test				
	MAE	RMSE	d	NSE	Max(RE)	MAE	RMSE	d	NSE	Max(RE)
ANN	11.289	14.517	0.893	0.791	41.956	19.177	24.319	0.751	0.521	50.399
ANN-PSO	11.248	14.470	0.894	0.791	41.760	19.174	24.286	0.751	0.521	50.170
ANN-HS	8.460	10.804	0.920	0.843	25.528	18.038	22.362	0.746	0.549	41.441
ANN-ADHS	4.535	5.850	0.958	0.916	15.800	14.784	17.871	0.803	0.630	32.836

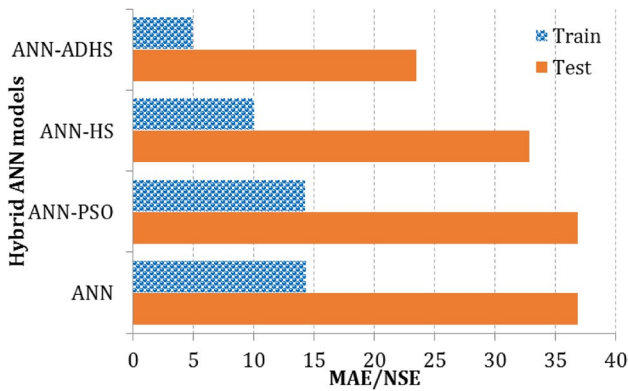
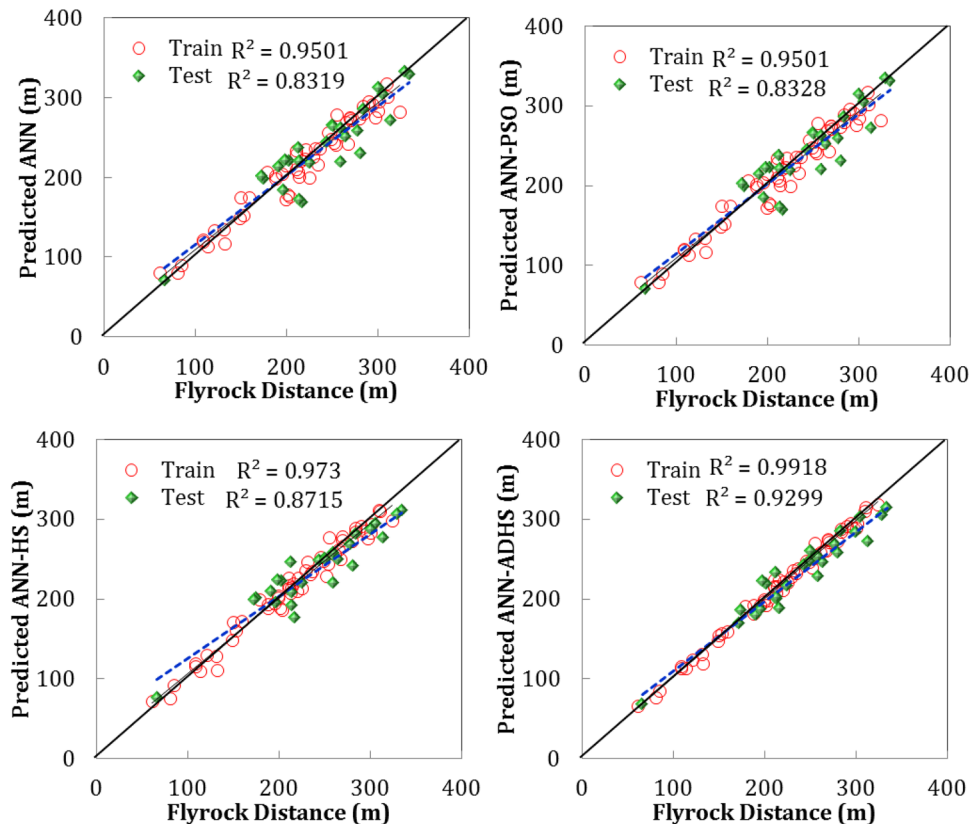


**Fig. 7** MAE/NSE ratio of different ANN models in the training and testing phases

varies from 0 to 1 with no-correlation with the perfect fitness. The *NSE* in Eq. (12) presents the goodness-of-fitness of the model, where  $NSE = 1$  indicates perfect agreement predictions. If Max (RE) is close to zero, then the predicted results using an AI-based model show the highest tendency.

Three optimization algorithms based on the training approach of ANN coupled with HS, PSO, and the proposed ADHS are compared in Fig. 6. In this figure, MSE is plotted corresponding to the iteration of different optimization methods. It can be given from Fig. 6, the MSE of PSO and HS are provided similar to a value of 0.023. However, the ADHS shows the lowest MSE (0.006). This clearly shows the superiority of ADHS compared to PSO and HS algorithms. In addition, the highly convergence rate is obtained

**Fig. 8** Scatterplot of different ANN models in the training and testing phases





using the adjusting process proposed by the dynamical adaptive formulation in ANN-based ADHS optimization procedure. Two dynamical adjusting processes in ANN-ADHS extracted from the information of harmony elements can provide acceptable weights and biases compared to ANN-PSO and ANN-HS.

The performances of different hybrid intelligent models, i.e., ANN-PSO, ANN-HS, and ANN-SDHS in terms

of accuracy (i.e., the lowest MAE and RMSE), tendency (i.e., the lowest Max (RE)), and agreement (i.e., the highest d and NSE) are compared for the testing and training database in Table 2. It is worth mentioning that 56 and 26 datasets were used in training and testing phases, respectively. Table 2 shows that the lowest MAE, RMSE, and Max (RE) values were obtained by the ANN-ADHS model. In addition, the highest d and NSE values were also obtained from

**Fig. 9** Observed and predicted results of the samples in the testing and training phases

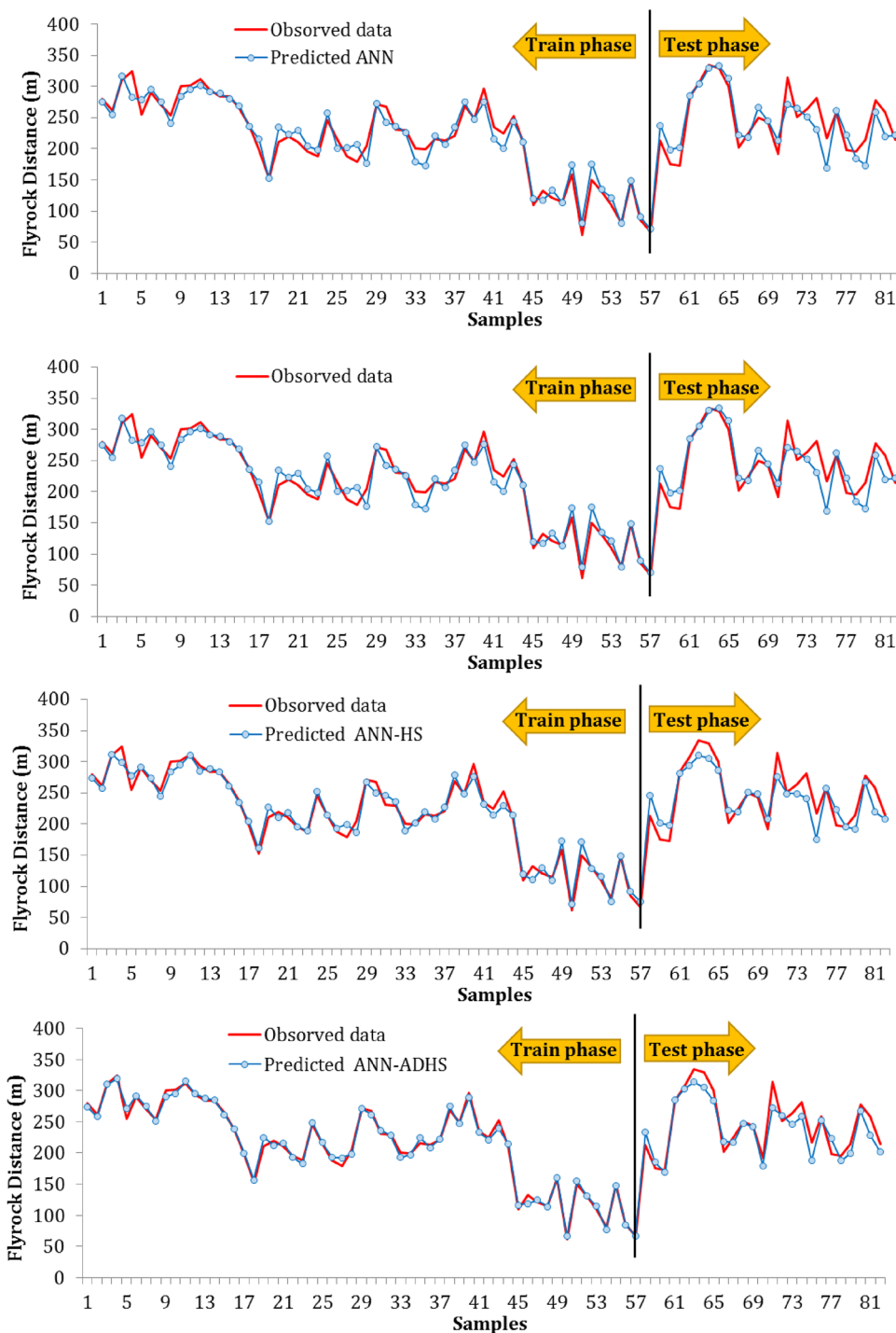
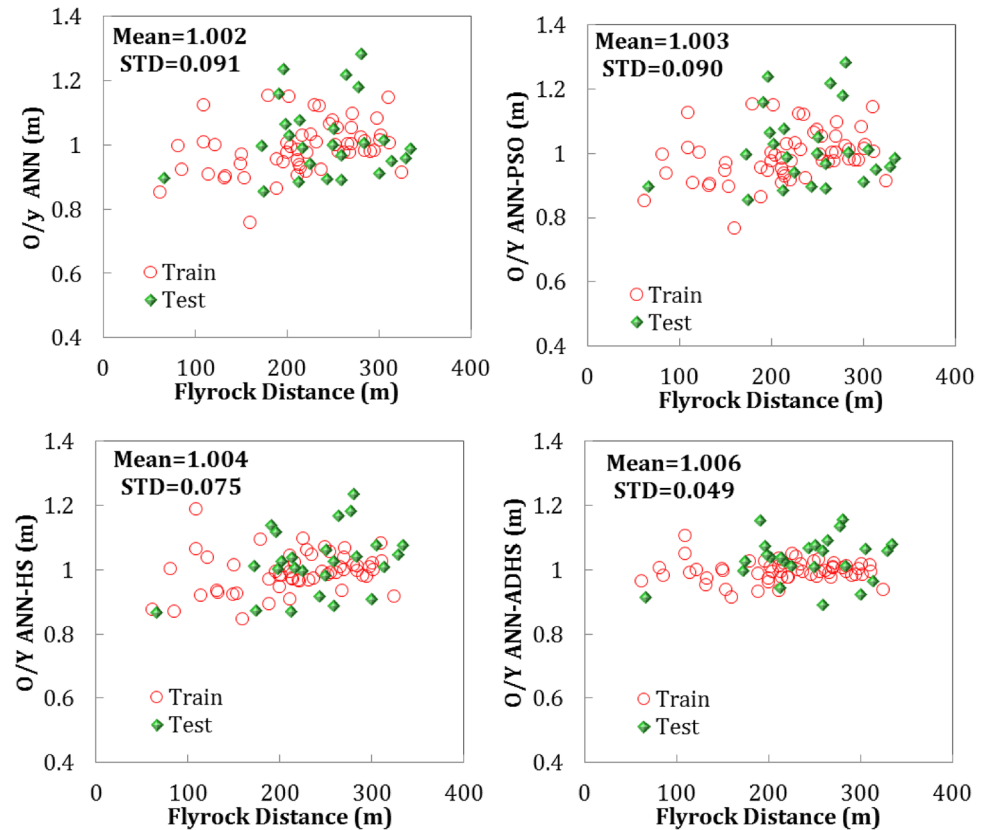


**Fig. 10** Uncertainty (O/Y) of different models



the ANN-ADHS model. These values clearly indicated the superiority of the ANN-ADHS model in predicting flyrock compared to the others.

To more reliably compare the prediction performance of the models, the MAE to NSE ratios (MAE/NSE) were compared for different ANN models trained by the traditional algorithm, HS, PSO, and ADHS. The lowest MAE/NSE shows the model with the best level of accuracy and agreement. The MAE/NSE ratios for different BP optimization methods are plotted in Fig. 7 for both training and testing predicted data. Generally, the MAE/NSE for ANN, ANN-HS, and ANN-PSO showed similar values for both testing and training phases. According to Fig. 7, the ANN-ADHS provides the best predictions among the other models, while the ANN-HS shows the worst results. To evaluate the tendency of the proposed BP using ADHS in ANN model for flyrock prediction, the predicted results with respect to the observed flyrock is plotted and presented as scatter points for training and testing phases in Table 2. The correlation coefficient ( $R^2$ ) between the predicted and observed data was implemented to compare the obtained results. If  $R^2$  tends to 1, the predicted model provides the perfect prediction with top tendency. As can be seen in Fig. 8, the maximum  $R^2$  values for both training and testing phases were obtained by the ANN-ADHS model. In other words, the ANN-ADHS model outperformed the others in terms of flyrock prediction. The

ANN-HS, ANN-PSO, and ANN models were ranked next, respectively.

Furthermore, a view of the predicted flyrock values for all 82 datasets (both training and testing phases) using all the predictive models is illustrated in Fig. 9. According to this figure, the ANN-ADHS model, with the  $R^2$  of 0.991 and 0.929 in training and testing phases, respectively, was found as the most accurate model in predicting the flyrock in the cases studied in this paper. The ratios of the uncertainties of the predicted ANN models to the predicted data of flyrock distance (O/Y) are presented in Fig. 10. The average (Mean) and standard deviation (STD) are presented in Fig. 10 for the investigated models. In general, the model has a perfect prediction when STD and Mean are tended to 0 and 1, respectively. The model with the lowest STD can be introduced as a predictive model with the minimum uncertainty that can offer the most reliable prediction. As can be seen in Fig. 10, the proposed ANN-ADHS provides the lowest STD (0.049). This means that this model has the lowest uncertainty of predictions among the other models, i.e., ANN, ANN-HS, and ANN-PSO. The HS-based training algorithm of ANN shows a STD value (0.075) better than that of ANN (0.091) and ANN-PSO (0.09).

## 5 Conclusion

Control of the flyrock induced by blasting is always a challenge for engineers working in surface mines. The aim of this study is to propose a novel and accurate model, namely the ANN-ADHS model, for flyrock prediction. To the best of our knowledge, no research has tested the efficiency of the ANN-ADHS model in terms of predicting flyrock in different time scales as yet. To achieve the objectives defined for this research, three quarry sites located near the city of Johor, Malaysia, were investigated and the required datasets were measured. The predictive models were first trained using 56 datasets and then tested and verified using 26 datasets. After the modeling process, the performance of the models was evaluated using five comparative statistics, i.e., MAE, RMSE,  $d$ , NSE, and  $R^2$ . The conclusions of this study are as follow:

- The ANN-ADHS model was found superior to the other models investigated in this study (i.e., ANN-HS, ANN-PSO, and ANN) regarding the prediction of flyrock.  $R^2$  of testing in ANN-ADHS model was about 0.93, while that value of ANN-HS, ANN-PSO, and ANN models were about 0.871, 0.832, and 0.831, respectively. Accordingly, the ANN-ADHS model was found capable of providing greatest accuracy in the field of flyrock prediction.
- The ADHS was found a powerful algorithm for improving the ANN performance, and also it showed its high capacity for being generalized.
- The ANN-ADHS model proposed in this study can be applied to predicting other blasting impacts such as ground vibration and air overpressure.

**Acknowledgements** The authors are grateful to Dr. Danial Jahed Armaghani for providing the information and facilities required for conducting this research.

## References

1. Trivedi R, Singh TN, Mudgal K (2014) Impact of geotechnical parameters on blast induced flyrocks using artificial neural network—a case study. In: Proceedings of 2nd international conference on advanced technology in exploration and exploitation of minerals, advance Minetech. Jodhpur, India, pp 128–134
2. Jahed Armaghani D, Hajihassani M, Mohamad ET, Marto A, Noorani SA (2014) Blasting-induced flyrock and ground vibration prediction through an expert artificial neural network based on particle swarm optimization. *Arab J Geosci* 7:5383–5396
3. Trivedi R, Singh TN, Gupta N (2015) Prediction of blast-induced flyrock in opencast mines using ANN and ANFIS. *Geotech Geol Eng* 33:875–891
4. Zhang J, Xiao M, Gao L, Chu S (2019) Probability and interval hybrid reliability analysis based on adaptive local approximation of projection outlines using support vector machine. *Comput Aided Civil Infrastruct Eng* 34(11):991–1009
5. Hasanipanah M, Faradonbeh RS, Armaghani DJ, Amnieh HB, Khandelwal M (2017) Development of a precise model for prediction of blast-induced flyrock using regression tree technique. *Environ Earth Sci* 76(1):27
6. Hasanipanah M, Shahnazar A, Amnieh HB, Armaghani DJ (2017) Prediction of air-overpressure caused by mine blasting using a new hybrid PSO–SVR model. *Eng Comput* 33(1):23–31
7. Hasanipanah M, Bakhshandeh Amnieh H, Arab H, Zamzam MS (2018) Feasibility of PSO–ANFIS model to estimate rock fragmentation produced by mine blasting. *Neural Comput Appl* 30(4):1015–1024
8. Zhou J, Li C, Arslan CA, Hasanipanah M, Amnieh HB (2019) Performance evaluation of hybrid FFA–ANFIS and GA–ANFIS models to predict particle size distribution of a muck-pile after blasting. *Eng Comput*. <https://doi.org/10.1007/s00366-019-00822-0>
9. Keshtegar B, Hasanipanah M, Bakhshayeshi I, Sarafraz ME (2019) A novel nonlinear modeling for the prediction of blast induced airblast using a modified conjugate FR method. *Measurement* 131:35–41
10. Hasanipanah M, Amnieh HB (2020) Developing a new uncertain rule-based fuzzy approach for evaluating the blast-induced back-break. *Eng Comput*. <https://doi.org/10.1007/s00366-019-00919-6>
11. Nguyen H, Bui X, Tran Q et al (2020) A comparative study of empirical and ensemble machine learning algorithms in predicting air over-pressure in open-pit coal mine. *Acta Geophys* 68:325–336. <https://doi.org/10.1007/s11600-019-00396-x>
12. Little TN, Blair DP (2009) Mechanistic Monte Carlo models for analysis of flyrock risk. In: Proceedings of the 9th international symposium on rock fragmentation by blasting, Granada, Spain, pp 641–647
13. Raina AK, Chakraborty AK, Choudhury PB, Siha A (2011) Flyrock danger zone demarcation in opencast mines: a risk based approach. *Bull Eng Geol Environ* 70:163–172
14. Adhikari GR (1999) Studies on flyrock at limestone quarries. *Rock Mech Rock Eng* 32(4):291–301
15. Rehak TR, Bajpayee TS, Mowrey GL, Ingram DK (2001) Flyrock issues in blasting. In: Proceedings of the 27th annual conference on explosives and blasting technique. vol 1. International Society of Explosives Engineers, Cleveland, pp 165–175
16. Bajpayee TS, Rehak TR, Mowrey GL, Ingram DK (2000) A summary of fatal accidents due to flyrock and lack of blast area security in surface mining, 1989–1999. In: Proceedings of 28th annual conference on explosives and blasting technique. International Society of Explosives Engineers, 10–13 Feb 2000, NIOSH, Las Vegas, Nevada, pp 105–188
17. Bajpayee TS, Rehak TR, Mowrey GL, Ingram DK (2004) Blasting injuries in surface mining with emphasis on flyrock and blast area security. *J Saf Res* 35:47–57
18. Richards AB, Moore AJ (2004) Flyrock control—by chance or design. In: Proceedings of 30th annual conference on explosives and blasting technique. International Society of Explosive Engineers, New Orleans, Louisiana USA, pp 335–348
19. Verakis HC, Lobb TE (2003) An analysis of blasting accidents in mining operations. In: Proceedings of the 29th annual conference on explosives and blasting technique, 2 Cleveland, OH: International Society of Explosives Engineers, pp 119–129
20. Kecojevic V, Radomsky M (2005) Flyrock phenomena and area security in blasting-related accidents. *Saf Sci* 43:739–750
21. CSIR-CIMFR (2014) Prediction and control of flyrock hazards due to blasting in opencast mines using artificial neural network. Interim report, Grant in Aid Project (GAP/87/EMG/DST/2010-11) Central Institute of Mining and Fuel Research, Dhanbad, India

22. Workman JL, Calder PN (1994) Flyrock prediction and control in surface mine blasting. In: Proceedings of 20th annual conference on explosives and blasting technique, Austin, Texas, Cleveland, OH: International Society of Explosives Engineers, pp 59–74
23. Monjezi M, Hasanipanah M, Khandelwal M (2013) Evaluation and prediction of blast-induced ground vibration at Shur River Dam, Iran, by artificial neural network. *Neural Comput Appl* 22(7–8):1637–1643
24. Nikafshan Rad H, Jalali Z, Jalalifar H (2015) Prediction of rock mass rating system based on continuous functions using Chaos–ANFIS model. *Int J Rock Mech Min Sci* 73:1–9
25. Hasanipanah M, Armaghani DJ, Amnieh HB, Majid MZA, Tahir MMD (2017) Application of PSO to develop a powerful equation for prediction of flyrock due to blasting. *Neural Comput Appl* 28(1):1043–1050
26. Shahnazar A, Nikafshan Rad H, Hasanipanah M, Tahir MM, Armaghani DJ, Ghoroghi M (2017) A new developed approach for the prediction of ground vibration using a hybrid PSO-optimized ANFIS-based model. *Environ Earth Sci* 76(15):527
27. Zhang J, Gao L, Xiao M (2020) A new hybrid reliability-based design optimization method under random and interval uncertainties. *Int J Numer Meth Eng*. <https://doi.org/10.1002/nme.6440>
28. Amiri M, Hasanipanah M, Amnieh HB (2019) Predicting ground vibration induced by rock blasting using a novel hybrid of neural network and itemset mining. *Neural Comput Appl*. <https://doi.org/10.1007/s00521-020-04822-w>
29. Zhou J, Li E, Yang S, Wang M, Shi X, Yao S, Mitri HS (2019) Slope stability prediction for circular mode failure using gradient boosting machine approach based on an updated database of case histories. *Saf Sci* 118:505–518
30. Zhang Y, Gao L, Xiao M (2020) Maximizing natural frequencies of inhomogeneous cellular structures by Kriging-assisted multi-scale topology optimization. *Comput Struct* 230:106197
31. Zhou J, Li C, Arslan CA, Hasanipanah M, Amnieh HB (2019) Performance evaluation of hybrid FFA-ANFIS and GA-ANFIS models to predict particle size distribution of a muck-pile after blasting. *Eng Comput*. <https://doi.org/10.1007/s00366-019-00822-0>
32. Zhou J, Nekouie A, Arslan CA, Pham BT, Hasanipanah M (2019) Novel approach for forecasting the blast induced AOp using a hybrid fuzzy system and firefly algorithm. *Eng Comput*. <https://doi.org/10.1007/s00366-019-00725-0>
33. Asteris PG, Apostolopoulou M, Skentou AD, Antonia Moropoulou A (2019) Application of artificial neural networks for the prediction of the compressive strength of cement-based mortars. *Comput Concr* 24(4):329–345
34. Xiao M, Zhang J, Gao L, Lee S, Eshghi AT (2019) An efficient Kriging-based subset simulation method for hybrid reliability analysis under random and interval variables with small failure probability. *Struct Multidisciplin Optimiz* 59(6):2077–2092
35. Nikafshan Rad H, Hasanipanah M, Rezaei M, Eghlim AL (2019) Developing a least squares support vector machine for estimating the blast-induced flyrock. *Eng Comput* 34(4):709–717
36. Gao L, Xiao M, Shao X, Jiang P, Nie L, Qiu H (2012) Analysis of gene expression programming for approximation in engineering design. *Struct Multidisciplin Optimiz* 46(3):399–413. <https://doi.org/10.1007/s00158-012-0767-7>
37. Jing H, Rad HN, Hasanipanah M, Armaghani DJ, Qasem SN (2020) Design and implementation of a new tuned hybrid intelligent model to predict the uniaxial compressive strength of the rock using SFS-ANFIS. *Eng Comput*. <https://doi.org/10.1007/s00366-020-00977-1>
38. Ye J, Dalle J, Nezami R, Hasanipana M, Armaghani Jahed (2020) Stochastic fractal search-tuned ANFIS model to predict blast-induced air overpressure. *Eng Comput*. <https://doi.org/10.1007/s00366-020-01085-w>
39. Hasanipanah M, Zhang W, Armaghani DJ, Rad HN (2020) The potential application of a new intelligent based approach in predicting the tensile strength of rock. *IEEE Access* 8:57148–57157
40. Nauck D, Kruse R (1999) Obtaining interpretable fuzzy classification rules from medical data. *Artif Intell Med* 16:149–169
41. Rezaei M, Monjezi M, Varjani AY (2011) Development of a fuzzy model to predict flyrock in surface mining. *Saf Sci* 49(2):298–305
42. Ghasemi E, Amini H, Ataei M, Khalokakaei R (2014) Application of artificial intelligence techniques for predicting the flyrock distance caused by blasting operation. *Arab J Geosci* 7:193–202
43. Monjezi M, Khoshalan HA, Varjani AY (2012) Prediction of flyrock and backbreak in open pit blasting operation: a neurogenetic approach. *Arab J Geosci* 5:441–448
44. Khandelwal M, Monjezi M (2013) Prediction of flyrock in open pit blasting operation using machine learning method. *Int J Rock Mech Min Sci* 23:313–316
45. Marto A, Hajihassani M, Jahed Armaghani D, Tonnizam Mohamad E, Makhtar AM (2014) A novel approach for blast induced flyrock prediction based on imperialist competitive algorithm and artificial neural network. *Sci World J* 5:643715
46. Jahed Armaghani D, Mohamad ET, Hajihassani M, Abad SANK, Marto A, Moghaddam MR (2015) Evaluation and prediction of flyrock resulting from blasting operations using empirical and computational methods. *Eng Comput*. <https://doi.org/10.1007/s00366-015-0402-5>
47. Nikafshan Rad H, Bakhshayeshi I, Wan Jusoh WA, Tahir MM, Kok Foong L (2019) Prediction of flyrock in mine blasting: a new computational intelligence approach. *Nat Resour Res*. <https://doi.org/10.1007/s11053-019-09464-x>
48. Lu X, Hasanipanah M, Brindhadevi K et al (2020) ORELM: a novel machine learning approach for prediction of flyrock in mine Blasting. *Nat Resour Res* 29:641–654
49. Murlidhar BR, Kumar D, Jahed Armaghani D et al (2020) A novel intelligent ELM-BBO technique for predicting distance of mine blasting-induced flyrock. *Nat Resour Res*. <https://doi.org/10.1007/s11053-020-09676-6>
50. Han H, Jahed Armaghani D, Tarinejad R et al (2020) Random forest and bayesian network techniques for probabilistic prediction of flyrock induced by blasting in quarry sites. *Nat Resour Res* 29:655–667
51. Zhou J, Aghili N, Ghaleini EN et al (2020) A Monte Carlo simulation approach for effective assessment of flyrock based on intelligent system of neural network. *Eng Comput* 36:713–723
52. Hudaverdi T, Akyildiz O (2019) A new classification approach for prediction of flyrock throw in surface mines. *Bull Eng Geol Environ* 78:177–187
53. Armaghani DJ, Koopialipour M, Bahri M et al (2020) A SVR-GWO technique to minimize flyrock distance resulting from blasting. *Bull Eng Geol Environ*. <https://doi.org/10.1007/s10064-020-01834-7>
54. Hornik K, Stinchcombe M, White H (1989) Multilayer feedforward networks are universal approximators. *Neural Networks* 2:359–366
55. Mirjalili S, Hashim SZM, Sardroudi HM (2012) Training feedforward neural networks using hybrid particle swarm optimization and gravitational search algorithm. *Appl Math Comput* 218:11125–11137
56. Khatir S, Tiachacht S, Thanh CL, Bui TQ, Wahab MA (2019) Damage assessment in composite laminates using ann-pso-iga and cornwell indicator. *Compos Struct* 230:111509
57. Zhang J, Xiao M, Gao L (2019) A new method for reliability analysis of structures with mixed random and convex variables. *Appl Math Model* 70:206–220
58. Ojha VK, Abraham A, Snášel V (2017) Metaheuristic design of feedforward neural networks: a review of two decades of research. *Eng Appl Artif Intell* 60:97–116



59. Keshtegar B, Heddami S, Hosseinabadi H (2019) The employment of polynomial chaos expansion approach for modeling dissolved oxygen concentration in river. *Environ Earth Sci* 78:34
60. Keshtegar B, Kisi O (2018) RM5Tree: radial basis M5 model tree for accurate structural reliability analysis. *Reliabil Eng Syst Saf* 180:49–61
61. Keshtegar B, Heddami S (2018) Modeling daily dissolved oxygen concentration using modified response surface method and artificial neural network: a comparative study. *Neural Comput Appl* 30:2995–3006
62. Keshtegar B, Heddami S, Sebbar A, Zhu S-P, Trung N-T (2019) SVR-RSM: a hybrid heuristic method for modeling monthly pan evaporation. *Environ Sci Pollut Res* 26:35807–35826
63. Zhang J, Xiao M, Gao L, Fu J (2018) A novel projection outline based active learning method and its combination with Kriging metamodel for hybrid reliability analysis with random and interval variables. *Comput Methods Appl Mech Eng* 341:32–52
64. Zhu SP, Keshtegar B, Chakraborty S, Trung NT (2020) Novel probabilistic model for searching most probable point in structural reliability analysis. *Comput Methods Appl Mech Eng* 366:113027
65. Seghier MEAB, Keshtegar B, Tee KF, Zayed T, Abbassi R, Trung NT (2020) Prediction of maximum pitting corrosion depth in oil and gas pipelines. *Eng Fail Anal* 112:104505
66. Keshtegar B, Gholampour A, Ozbakkaloglu T, Zhu SP, Trung NT (2020) Reliability analysis of FRP-confined concrete at ultimate using conjugate search direction method. *Polymers* 12(3):707
67. Zhang J, Xiao M, Gao L, Chu S (2019) A combined projection-outline-based active learning Kriging and adaptive importance sampling method for hybrid reliability analysis with small failure probabilities. *Comput Methods Appl Mech Eng* 344:13–33
68. Keshtegar B, Bagheri M, Meng D, Kolahchi R, Trung NT (2020) Fuzzy reliability analysis of nanocomposite ZnO beams using hybrid analytical-intelligent method. *Eng Comput*. <https://doi.org/10.1007/s00366-020-00965-5>
69. Keshtegar B, Meng D, Ben Seghier MEA, Xiao M, Trung N-T, Bui DT (2020) A hybrid sufficient performance measure approach to improve robustness and efficiency of reliability-based design optimization. *Eng Comput*. <https://doi.org/10.1007/s00366-019-00907-w>
70. Hasanipanah M, Bakhshandeh Amnieh H (2020) A fuzzy rule based approach to address uncertainty in risk assessment and prediction of blast-induced flyrock in a quarry. *Nat Resour Res*. <https://doi.org/10.1007/s11053-020-09616-4>
71. Xiao M, Zhang J, Gao L (2020) A system active learning Kriging method for system reliability-based design optimization with a multiple response model. *Reliabil Eng Syst Saf* 199:106935. <https://doi.org/10.1016/j.res.2020.106935>
72. Heddami S, Keshtegar B, Kisi O (2020) Predicting total dissolved gas concentration on a daily scale using kriging interpolation, response surface method and artificial neural network: case study of Columbia River Basin Dams, USA. *Nat Resour Res* 29:1801–1818

**Publisher's Note** Springer Nature remains neutral with regard to jurisdictional claims in published maps and institutional affiliations.